Polynomial approach for modeling a piezoelectric disc resonator partially covered with electrodes

L. Elmaimouni, Jean-Etienne Lefebvre, F.E. Ratolojanahary, J.G. Yu, P.M. Rabotovao, I. Naciri, Tadeusz Gryba, Mohamed Rguiti

*

Polynomial approach for modeling a piezoelectric disk resonator partially covered with electrodes

L. Elmaimouni[2,*], J. E. Lefebvre[1,3], F. E. Ratolojanahary[4], J.G. Yu[5], P. M. Rabotovao[4]

I. Naciri[2,6], T. Gryba[1,3] and M. Rguiti[1,7]

[1] *Univ Lille Nord de France, F-59000 Lille, France*

[2] *LSIE-ERMAM, Faculté polydisciplinaire d'Ouarzazate, Univ. Ibn Zohr, 45000 Ouarzazate, Maroc*

[3] *IEMN, UMR CNRS 8520, Département OAE, UVHC, 59313-Valenciennes Cedex 9, France*

[4] *LAPAUF, Université de Fianarantsoa, 301 Fianarantsoa, Madagascar*

[5] *School of Mechanical & Power Engineering, Henan Polytechnic Univ, Jiaozuo, 454003, China*

[6] *Faculté des Sciences d'Agadir, Univ. Ibn Zohr, BP.28/S Agadir, Maroc*

[7] *UVHC, LMCPA, F-59600 Maubeuge, France*

[*]Telephone: +212.5.24.88.57.98; mobile phone: +212.6.15.13.05.84, fax: +212.5.24.88.58.01

Email address: [*]la_elmaimouni@yahoo.fr

Abstract: The frequency spectrum of a partially piezoelectric disc resonator is studied by using Legendre polynomials. The formulation, based on three dimensional equations of linear elasticity, takes into account the high contrast between the electroded and non-electroded regions. The mechanical displacement components and the electrical potential are expanded in a double series of orthonormal functions and are introduced into the equations governing wave propagation in piezoelectric media. The boundary and continuity conditions are automatically incorporated into the equations of motion by assuming position-dependent material physical constants or delta-functions. The incorporation of electrical sources is illustrated. Structure symmetry was used to reduce the number of unknowns. The vibration characteristics of piezoelectric discs are analyzed by the three dimensional modelling

approach with the modal and harmonic analyses. Numerical results are presented such as resonant and anti-resonant frequencies, electric input admittance, electromechanical coupling coefficient and field profiles for PIC151 and PZT5A resonator discs fully and partially metallized. The results obtained are compared with those published earlier and those obtained from an analytical approach in order to validate our model.

Keywords: *Legendre Polynomial, Fully and partially electroded piezoelectric resonator disc, Contour-mode resonators, MEMS resonators, Acoustic wave, Input electrical admittance, Resonant and Anti-resonant frequencies, Electromechanical Coupling Coefficient.*

1. INTRODUCTION

Micro-electro-mechanical systems (MEMS) resonators are rapidly gaining importance as they are spreading more and more into many different fields of applications, for example transportation, communication, automated manufacturing, environmental monitoring, health care, defense systems, and a wide range of consumer products [1-7]. Among the different types of MEMS, resonantly driven micro-devices are an important branch that requires the analysis of the resonant and anti-resonant frequencies and the modal shapes of the structure [8].

The vibration characteristics of piezoelectric structures are completely determined from the three dimensional equations of linear elasticity, the Maxwell equations, and the piezoelectric constitutive equations [9, 10]. There are many studies which deal with modelling of the MEMS piezoelectric resonator. Guo et al [11] presented and calculated the resonant frequencies for PZT-5A piezoelectric discs with diameter-to-thickness ratios of 20 and 10 using the vibrations characteristics of piezoelectric discs. Ivina [12] analysed the thickness

symmetric vibrations of piezoelectric discs with partial axi-symmetric electrodes by using the finite element method. Schmidt [13] employed the linear piezoelectric equations to investigate the extensional vibrations of a thin partly electroded piezoelectric plate. Rogacheva [14] used the cases of piezoceramic discs and cylindrical shells based on the finite element method to analyse and calculate the resonant and anti-resonant frequencies and electromechanical coupling coefficient. Chi-Hung Huang [15] analyzed a thin piezoceramic disc partially covered with electrodes using the linear theoretical and experimental vibration.

In the literature, several methods are used for modelling the acoustic propagation in a piezoelectric structure. Among these methods, the Legendre polynomial method provides excellent precision for the waveguides with various geometries such as planar and cylindrical multilayered and functionally graded structures [16-19]. This method uses constitutive and propagation equations to describe the structure; it is easy to implement for numerical calculations, with remarkable simplicity when using physical quantities such as elastic stiffness, permittivity and density along with rectangular window functions through which the boundary conditions are automatically included [20-22]. Moreover, the acoustic field distributions are easily obtained [23-25]. However, (i) it has only been applied to modelling Bulk Acoustic Wave (BAW) resonators in plates [26-28], and never for analyzing partially electroded cylindrical resonators; (ii) its convergence depends on the relative properties of the materials.

In this paper, as announced in the perspective of a previous paper [25], we present a polynomial approach for studying the frequency spectrum of a partially electroded piezoelectric MEMS resonator disc. The formulation statement is based on linear three-dimensional elasticity using an analytic form for the field variables. The boundary, symmetry, and continuity conditions according to the geometry of the structure are automatically incorporated into the physical equations that govern the structure. The incorporation of the

electrical source in the field equations is illustrated. The numerical results for harmonic and modal analyses are presented for a full and a partial metallization. To take into account the high contrast between the electroded and non-electroded regions, the structure studied is divided into two parts: the electroded one and the non-electroded one. Resonant and anti-resonant frequencies, electric input admittance (impedance), electromechanical coupling coefficient and field profiles, easily obtained, are presented for PIC151 and PZT5A. The results obtained are, for extreme geometries allowing a one-dimensional approached analytical modelling, compared with those obtained by the approached analytical model. A good agreement is obtained.

2. Mathematics and formulation of the problem

Consider a homogeneous solid cylinder of finite height assumed to have undergone a uniform polarization treatment in the thickness direction. R and H are respectively the radius and thickness of the cylinder. Assume that the crystalline z-axis coincides with the axis of the disc taken as the z-axis of a cylindrical coordinate system $Or\phi z$. The polarization is in the z direction and the faces at $z=\pm H/2$ of the disc are covered with central electrodes of radius R_0. The electrodes on top and bottom surfaces are assumed to be very thin and their mechanical properties such as mass and stiffness are assumed negligible. They are connected to a signal generator $V = V_0 e^{j\omega t}$ as shown in Fig.1.

We assume that the elastic and piezoelectric medium of the cylinder is characterized by constant mass density ρ, elastic moduli at constant electric field $\{C_{ij}\}$, piezoelectric constant $\{e_{ij}\}$ and electric permittivity at constant strain $\{\varepsilon_{ij}\}$ defined with respect to the coordinates axes $Or\phi z$. The strain-displacement relations are given by [29]:

$$\begin{aligned} S_{rr} &= \frac{\partial u}{\partial r} & 2S_{\phi z} &= \frac{\partial v}{\partial z} + \frac{1}{r}\frac{\partial w}{\partial \phi} \\ S_{\phi\phi} &= \frac{u}{r} + \frac{1}{r}\frac{\partial v}{\partial \phi} \quad ; & 2S_{rz} &= \frac{\partial u}{\partial z} + \frac{\partial w}{\partial r} \\ S_{zz} &= \frac{\partial w}{\partial z} & 2S_{r\phi} &= \frac{1}{r}\frac{\partial u}{\partial \phi} + \frac{\partial v}{\partial r} - \frac{v}{r} \end{aligned} \tag{1}$$

where u, v, and w are the mechanical displacement components respectively in the radial, circumferential, and axial directions. We assume the disc material has the symmetry of a hexagonal crystal in class 6mm.

The constitutive equations for a 6mm linear piezoelectric material can be expressed as:

$$\begin{cases} T_{rr} = C_{11}\frac{\partial u}{\partial r} + C_{12}(\frac{u}{r} + \frac{1}{r}\frac{\partial v}{\partial \phi}) + C_{13}\frac{\partial w}{\partial z} + e_{31}\frac{\partial \varphi}{\partial z} \\ T_{\phi\phi} = C_{12}\frac{\partial u}{\partial r} + C_{22}(\frac{u}{r} + \frac{1}{r}\frac{\partial v}{\partial \phi}) + C_{23}\frac{\partial w}{\partial z} + e_{31}\frac{\partial \varphi}{\partial z} \\ T_{zz} = C_{13}\frac{\partial u}{\partial r} + C_{23}(\frac{u}{r} + \frac{1}{r}\frac{\partial v}{\partial \phi}) + C_{33}\frac{\partial w}{\partial z} + e_{33}\frac{\partial \varphi}{\partial z} \\ T_{\phi z} = C_{44}(\frac{\partial v}{\partial z} + \frac{1}{r}\frac{\partial w}{\partial \phi}) + e_{15}\frac{\partial \varphi}{\partial \phi} \\ T_{rz} = C_{55}(\frac{\partial u}{\partial z} + \frac{\partial w}{\partial r}) + + e_{15}\frac{\partial \varphi}{\partial r} \\ T_{r\phi} = C_{66}(\frac{1}{r}\frac{\partial u}{\partial \phi} + \frac{\partial v}{\partial r} - \frac{v}{r}) \end{cases} \tag{2}$$

$$\begin{cases} D_r = e_{15}\left(\frac{\partial u}{\partial z} + \frac{\partial w}{\partial r}\right) - \varepsilon_{11}\frac{\partial \varphi}{\partial r} \\ D_\phi = e_{15}\left(\frac{\partial v}{\partial z} + \frac{1}{r}\frac{\partial w}{\partial \phi}\right) - \varepsilon_{11}\frac{\partial \varphi}{\partial \phi} \\ D_z = e_{31}\frac{\partial u}{\partial r} + e_{31}\left(\frac{u}{r} + \frac{1}{r}\frac{\partial v}{\partial \phi}\right) + e_{33}\frac{\partial w}{\partial z} - \varepsilon_{33}\frac{\partial \varphi}{\partial z} \end{cases} \tag{3}$$

where φ denotes the electric potential and $T = [T_{rr}, T_{\phi\phi}, T_{zz}, T_{\phi z}, T_{rz}, T_{r\phi}]$ and $\vec{D} = [D_r, D_\phi, D_z]$ are respectively the stress and electric displacement components.

In cylindrical coordinates, the field equations governing wave propagation in piezoelectric media are given by [29]:

$$\frac{\partial T_{rr}}{\partial r} + \frac{1}{r}\frac{\partial T_{r\phi}}{\partial \phi} + \frac{\partial T_{rz}}{\partial z} + \frac{T_{rr} - T_{\phi\phi}}{r} = \rho\frac{\partial^2 u}{\partial t^2} \tag{4a}$$

$$\frac{\partial T_{r\phi}}{\partial r}+\frac{1}{r}\frac{\partial T_{\phi\phi}}{\partial \phi}+\frac{\partial T_{\phi z}}{\partial z}+\frac{2}{r}T_{r\phi}=\rho\frac{\partial^2 v}{\partial t^2} \tag{4b}$$

$$\frac{\partial T_{rz}}{\partial r}+\frac{1}{r}\frac{\partial T_{\phi z}}{\partial \phi}+\frac{\partial T_{zz}}{\partial z}+\frac{T_{rz}}{r}=\rho\frac{\partial^2 w}{\partial t^2} \tag{4c}$$

$$\frac{1}{r}\frac{\partial(rD_r)}{\partial r}+\frac{1}{r}\frac{\partial D_\phi}{\partial \phi}+\frac{\partial D_z}{\partial z}=0 \tag{4d}$$

The structure and the electric source are axisymmetric. In this case, the wave fields do not depend on the azimuthal variable ϕ ($\Rightarrow \partial/\partial\phi = 0$).

Eq. (4b) and Eqs. (4a-4c-4d) are uncoupled and describe respectively the torsional modes ($u, w = 0, v \neq 0$) and the longitudinal modes ($u, w \neq 0, v = 0$). Moreover, the torsional modes cannot be excited electrically as, in Eq. (4b), the mechanical displacement v is uncoupled from the electric field for axisymmetric devices. So, we only take into account Eq. (4a), Eq. (4c), and Eq. (4d).

Both lateral and terminal surfaces are assumed to be stress free, so the normal component of the stress should be zero. At the outer lateral surface, the normal component D_r of the electrical displacement should be zero.

Now the changes of variables $q_1 = r/R$ and $q_3 = 2z/H$ are introduced for mathematical convenience.

Throughout this paper, we adopt variables: $\overline{u} = u(m)\times 10^{+10} = u(\text{Å})$, $\overline{v} = v(m)\times 10^{+10} = v(\text{Å})$, $\overline{w} = w(m)\times 10^{+10} = w(\text{Å})$, $\overline{T}_{ij} = T_{ij}/C_{33}^D$, $\overline{D}_k = D_k/\varepsilon_{33}$, and the normalized physical constants: $\overline{C}_{ij} = C_{ij}/C_{33}^D$, $\overline{e}_{ij} = e_{ij}/\sqrt{C_{33}^D\varepsilon_{33}}$, $\overline{\varepsilon}_{ij} = \varepsilon_{ij}/\varepsilon_{33}$ where $C_{33}^D = C_{33} + e_{33}^2/\varepsilon_{33}$ is the elastic stiffness constant at constant electric displacement. i, j and k take on the values 1,2 and 3.

The stress-displacement and the electric displacement relations for the extensional vibration in region (1) with electrodes and region (2) without electrodes are given respectively in Eqs. (5) and (6):

$$\begin{cases} \overline{T}_{rr}^{(i)} = \left(\overline{C}_{11} \dfrac{1}{R} \dfrac{\partial \overline{u}^{(i)}}{\partial q_1} + \overline{C}_{12} \dfrac{1}{R} \dfrac{\overline{u}^{(i)}}{q_1} + \overline{C}_{13} \dfrac{2}{H} \dfrac{\partial \overline{w}^{(i)}}{\partial q_3} + \overline{e}_{31} \dfrac{1}{\beta} \dfrac{2}{H} \dfrac{\partial \varphi^{(i)}}{\partial q_3} \right).10^{-10} \\ \overline{T}_{\phi\phi}^{(i)} = \left(\overline{C}_{12} \dfrac{1}{R} \dfrac{\partial \overline{u}^{(i)}}{\partial q_1} + \overline{C}_{11} \dfrac{\overline{u}^{(i)}}{Rq_1} + \overline{C}_{13} \dfrac{2}{H} \dfrac{\partial \overline{w}^{(i)}}{\partial q_3} + \overline{e}_{31} \dfrac{1}{\beta} \dfrac{2}{H} \dfrac{\partial \varphi^{(i)}}{\partial q_3} \right).10^{-10} \\ \overline{T}_{zz}^{(i)} = \left(\overline{C}_{13} \dfrac{1}{R} \dfrac{\partial \overline{u}^{(i)}}{\partial q_1} + \overline{C}_{13} \dfrac{\overline{u}^{(i)}}{Rq_1} + \overline{C}_{33} \dfrac{2}{H} \dfrac{\partial \overline{w}^{(i)}}{\partial q_3} + \overline{e}_{33} \dfrac{1}{\beta} \dfrac{2}{H} \dfrac{\partial \varphi^{(i)}}{\partial q_3} \right).10^{-10} \\ \overline{T}_{rz}^{(i)} = \left(\overline{C}_{55} \left(\dfrac{2}{H} \dfrac{\partial \overline{u}^{(i)}}{\partial q_3} + \dfrac{1}{R} \dfrac{\partial \overline{w}^{(i)}}{\partial q_1} \right) + \overline{e}_{15} \dfrac{1}{\beta} \dfrac{1}{R} \dfrac{\partial \varphi^{(i)}}{\partial q_1} \right).10^{-10} \end{cases} \tag{5}$$

$$\begin{cases} \overline{D}_{q_1}^{(i)} = \overline{e}_{15} \dfrac{2\beta}{H} \dfrac{\partial \overline{u}^{(i)}}{\partial q_3} + \overline{e}_{15} \dfrac{\beta}{R} \dfrac{\partial \overline{w}^{(i)}}{\partial q_1} - \overline{\varepsilon}_{11} \dfrac{1}{R} \dfrac{\partial \varphi^{(i)}}{\partial q_1} \\ \overline{D}_{q_3}^{(i)} = \overline{e}_{31} \dfrac{\beta}{R} \dfrac{\partial \overline{u}^{(i)}}{\partial q_1} + \overline{e}_{31} \dfrac{\beta}{R} \dfrac{1}{q_1} \overline{u}^{(i)} + \overline{e}_{33} \dfrac{2\beta}{H} \dfrac{\partial \overline{w}^{(i)}}{\partial q_3} - \overline{\varepsilon}_{33} \dfrac{2}{H} \dfrac{\partial \varphi^{(i)}}{\partial q_3} \end{cases} \tag{6}$$

where the superscript (i) denotes the region number, $\varphi^{(i)}$ the electric potential with the usual quasi-static approximation, $\overline{T}_{ij}^{(i)}$ and $\overline{D}_{k}^{(i)}$ the normalized components of stress and electrical displacement in regions (1) and (2) with $\beta = 10^{-10}\sqrt{C_{33}^{D}/\varepsilon_{33}}$ (V.Å^{-1}).

The boundary and continuity conditions in the regions (1) and (2) of the piezoelectric resonator disc are given by:

- $T_{rr}^{(2)}(q_1 = a_0) = T_{rr}^{(1)}(q_1 = a_0)$; $T_{rz}^{(2)}(q_1 = a_0) = T_{rz}^{(1)}(q_1 = a_0)$; $T_{rz}^{(1)}(q_3 = \pm 1) = 0$
- $T_{rz}^{(2)}(q_3 = \pm 1) = 0$; $T_{zz}^{(1)}(q_3 = \pm 1) = 0$; $T_{zz}^{(2)}(q_3 = \pm 1) = 0$; $T_{rr}^{(2)}(q_1 = +1) = 0$
- $T_{rz}^{(2)}(q_1 = +1) = 0$; $D_{q_1}^{(2)}(q_1 = a_0) = D_{q_1}^{(1)}(q_1 = a_0)$; $D_{q_3}^{(2)}(q_3 = \pm 1) = 0$; $D_{q_1}^{(2)}(q_1 = 1) = 0$

where $a_0 = R_0 / R$ denotes the metallization rate.

We automatically incorporate the boundary conditions by introducing the functions $\theta(q_1)$ and $\pi(q_3)$, defined as follows:

$$\theta(q_1) = \begin{cases} 1 & if \quad 0 \le q_1 \le 1 \\ 0 & otherwise \end{cases} \quad ; \quad \pi(q_3) = \begin{cases} 1 & if \quad -1 \le q_3 \le 1 \\ 0 & otherwise \end{cases} \tag{7}$$

In the propagation equations, the delta functions, $\delta(q_1 - 1)$ and $\left(\delta(q_3 + 1) - \delta(q_3 - 1)\right)$, coming from the derivatives of $\theta(q_1)$ and $\pi(q_3)$, multiplied by the normal stress components and

electrical displacement components allow to satisfy the boundary conditions in the studied cylindrical structure [16]. In this case, the field equations governing wave propagation in piezoelectric media in regions (1) and (2) are given by:

$$\frac{1}{R}\frac{\partial \overline{T}_{rr}^{(1)}}{\partial q_1}+\frac{2}{H}\frac{\partial \overline{T}_{rz}^{(1)}}{\partial q_3}+\frac{\overline{T}_{rr}^{(1)}-\overline{T}_{\phi\phi}^{(1)}}{Rq_1}+\frac{1}{R}\left(\overline{T}_{rr}^{(2)}-\overline{T}_{rr}^{(1)}\right)\delta(q_1-a_0)+\frac{2}{H}\overline{T}_{rz}^{(1)}\left[\delta(q_3+1)-\delta(q_3-1)\right]$$
$$=10^{-10}\frac{\rho}{C_{33}^{D}}\frac{\partial^2\overline{u}^{(1)}}{\partial t^2} \tag{8a}$$

$$\frac{1}{R}\frac{\partial \overline{T}_{rz}^{(1)}}{\partial q_1}+\frac{2}{H}\frac{\partial \overline{T}_{zz}^{(1)}}{\partial q_3}+\frac{\overline{T}_{rz}^{(1)}}{Rq_1}+\frac{1}{R}\left(\overline{T}_{rz}^{(2)}-\overline{T}_{rz}^{(1)}\right)\delta(q_1-a_0)+\frac{2}{H}\overline{T}_{zz}^{(1)}\left[\delta(q_3+1)-\delta(q_3-1)\right]$$
$$=10^{-10}\frac{\rho}{C_{33}^{D}}\frac{\partial^2\overline{w}^{(1)}}{\partial t^2} \tag{8b}$$

$$\frac{1}{Rq_1}\frac{\partial}{\partial q_1}\left(q_1\overline{D}_{q_1}^{(1)}\right)+\frac{2}{H}\frac{\partial \overline{D}_{q_3}^{(1)}}{\partial q_3}+\frac{1}{R}\left(\overline{D}_{q_1}^{(2)}-\overline{D}_{q_1}^{(1)}\right)\delta(q_1-a_0)=0 \tag{8c}$$

$$\frac{1}{R}\frac{\partial \overline{T}_{rr}^{(2)}}{\partial q_1}+\frac{2}{H}\frac{\partial \overline{T}_{rz}^{(2)}}{\partial q_3}+\frac{\overline{T}_{rr}^{(2)}-\overline{T}_{\phi\phi}^{(2)}}{Rq_1}+\frac{1}{R}\left(\overline{T}_{rr}^{(2)}-\overline{T}_{rr}^{(1)}\right)\delta(q_1-a_0)+\frac{2}{H}\overline{T}_{rz}^{(2)}\left[\delta(q_3+1)-\delta(q_3-1)\right]$$
$$-\frac{1}{R}\overline{T}_{rr}^{(2)}\delta(q_1-1)=10^{-10}\frac{\rho}{C_{33}^{D}}\frac{\partial^2\overline{u}^{(2)}}{\partial t^2} \tag{8d}$$

$$\frac{1}{R}\frac{\partial \overline{T}_{rz}^{(2)}}{\partial q_1}+\frac{2}{H}\frac{\partial \overline{T}_{zz}^{(2)}}{\partial q_3}+\frac{\overline{T}_{rz}^{(2)}}{Rq_1}+\frac{1}{R}\left(\overline{T}_{rz}^{(2)}-\overline{T}_{rz}^{(1)}\right)\delta(q_1-a_0)+\frac{2}{H}\overline{T}_{zz}^{(2)}\left[\delta(q_3+1)-\delta(q_3-1)\right]$$
$$-\frac{1}{R}\overline{T}_{rz}^{(2)}\delta(q_1-1)=10^{-10}\frac{\rho}{C_{33}^{D}}\frac{\partial^2\overline{w}^{(2)}}{\partial t^2} \tag{8e}$$

$$\frac{1}{Rq_1}\frac{\partial}{\partial q_1}\left(q_1\overline{D}_{q_1}^{(2)}\right)+\frac{2}{H}\frac{\partial \overline{D}_{q_3}^{(2)}}{\partial q_3}+\frac{1}{R}\left(\overline{D}_{q_1}^{(2)}-\overline{D}_{q_1}^{(1)}\right)\delta(q_1-a_0)+\frac{2}{H}\overline{D}_{q_3}^{(2)}\left[\delta(q_3+1)-\delta(q_3-1)\right]$$
$$-\frac{1}{R}\overline{D}_{q_1}^{(2)}\delta(q_1-1)=0 \tag{8f}$$

The mechanical displacement components $\overline{u}^{(i)}$ and $\overline{w}^{(i)}$ and the electrical potential $\varphi^{(i)}$ with $i=1,2$ in the regions (1) and (2) are expanded in a double series of orthonormal functions in q_1 and q_3 with an analytic form chosen to ensure some of the boundary, symmetry, and continuity conditions. Here, we can develop these variables in terms of the Legendre polynomials P_m's as:

In region (1):

$$\begin{cases} \overline{u}^{(1)}(q_1,q_3,t) = \sum_{mn} p_{m,2n}^{(q_1,1)}\ Q_m^{(1)}(q_1)\ Q_{2n}(q_3)\ e^{j\omega t} \\ \overline{w}^{(1)}(q_1,q_3,t) = \sum_{mn} p_{m,2n+1}^{(q_3,1)}\ Q_m^{(1)}(q_1)\ Q_{2n+1}(q_3)\ e^{j\omega t} \\ \varphi^{(1)}(q_1,q_3,t) = \left[\frac{V_0}{2}q_3^3 + (q_3^2-1)\sum_{mn} r_{m,2n+1}^{(1)}\ Q_m^{(1)}(q_1)\ Q_{2n+1}(q_3)\right] e^{j\omega t} \end{cases} \quad (9)$$

where $p_{m,n}^{(q_i,1)}(i=1\ and\ 3)$ and $r_{m,n}^{(1)}$ are the expansion coefficients respectively for the mechanical displacements components and the electrical potential. They are given respectively in Angstrom and volts. $Q_m^{(1)}(q_1) = \sqrt{\frac{2m+1}{a_0}}\ P_m\left(\frac{2q_1}{a_0}-1\right)$ and $Q_m(q_3) = \sqrt{\frac{2m+1}{2}}\ P_m(q_3)$ are the set of orthonormal polynomials in the intervals respectively $]0,a_0]$ and $[-1,+1]$. V_0 is a voltage applied to the resonator.

In region (2):

$$\begin{cases} \overline{u}^{(2)}(q_1,q_3,t) = \overline{u}^{(1)}(a_0,q_3,t) + (q_1-a_0)\sum_{mn} p_{m,2n}^{(q_1,2)}\ Q_m^{(2)}(q_1)\ Q_{2n}(q_3)\ e^{j\omega t} \\ \overline{w}^{(2)}(q_1,q_3,t) = \overline{w}^{(1)}(a_0,q_3,t) + (q_1-a_0)\sum_{mn} p_{m,2n+1}^{(q_3,2)}\ Q_m^{(2)}(q_1)\ Q_{2n+1}(q_3)\ e^{j\omega t} \\ \varphi^{(2)}(q_1,q_3,t) = \varphi^{(1)}(a_0,q_3,t) + (q_1-a_0)\sum_{mn} r_{m,2n+1}^{(2)}\ Q_m^{(2)}(q_1)\ Q_{2n+1}(q_3)\ e^{j\omega t} \end{cases} \quad (10)$$

The proposed expansions for the mechanical displacement components and the electric potential allow to impose the continuity at $q_1 = a_0$.

The expansion coefficients $p_{m,n}^{(q_i,2)}(i=1\ and\ 3)$ and $r_{m,n}^{(2)}$ are given respectively in Angstrom and volts. $Q_m^{(2)}(q_1) = \sqrt{\frac{2m+1}{1-a_0}}\ P_m\left(\frac{2q_1}{1-a_0} - \frac{1+a_0}{1-a_0}\right)$ and $Q_m(q_3) = \sqrt{\frac{2m+1}{2}}\ P_m(q_3)$ are the set of orthonormal polynomials in the intervals respectively $]a_0,+1]$ and $[-1,+1]$.

The solutions are sought in the form of series of orthonormal polynomials Q_m where we take advantage of the parity of the physical variables and of the $P_m's$.

In practice, the summation over the polynomials in equations (9) and (10) is truncated at some finite values $m = M$ and $n = N$ when higher order terms become essentially negligible. Substituting Eqs. (5) and (6) into Eqs. (8a) to (8f) and multiplying Eqs. (8a) and (8d) with $q_1^2 H^2$, and Eqs. (8b), (8c), (8e) and (8f) with $q_1 H^2$, taking account of the mechanical displacements and the electric field of Eqs. (9) and (10), multiplying each equation of the region (1) and region (2) respectively by $Q_j^{(*,1)}(q_1).Q_k^*(q_3).e^{-j\omega t}$ and $Q_j^{(*,2)}(q_1).Q_k^*(q_3).e^{-j\omega t}$ with j and k running from zero to respectively M and N; integrating over q_1 from zero to a_0 in region (1) with electrodes, and from a_0 to 1 in region (2) without electrodes, and q_3 from -1 to +1, and taking advantage of the orthonormality of the polynomials $Q_m^{(1)}(q_1)$, $Q_m^{(2)}(q_1)$ and $Q_m(q_3)$, we obtain a form of the system of $6\times(M+1)\times(N+1)$ linear equations with $6\times(M+1)\times(N+1)$ unknowns ($p_{m,n}^{(q_i,j)}$ and $r_{m,n}^{(j)}$ with $i = 1, 3$ and $j = 1,2$) with the normalized frequency Ω as parameter

$$\begin{cases} II_{mnjk}p_{m,n}^{(b)} + JJ_{mnjk}r_{m,n} + fr_{jk}V_0 = -\Omega^2 MM_{mnjk}p_{m,n}^{(b)} \\ GG_{mnjk}p_{m,n}^{(b)} + KK_{mnjk}r_{m,n} + f_{jk}^{2,5}V_0 = 0 \end{cases} \tag{11}$$

where $\Omega = \omega\left(\frac{\pi}{H}\sqrt{C_{33}^D/\rho}\right)^{-1}$, $p_{m,n}^{(b)} = \begin{bmatrix} p_{m,2n}^{(q_1,1)} \\ p_{m,2n+1}^{(q_3,1)} \\ p_{m,2n}^{(q_1,2)} \\ p_{m,2n+1}^{(q_3,2)} \end{bmatrix}$; $r_{m,n} = \begin{bmatrix} r_{m,2n+1}^{(1)} \\ r_{m,2n+1}^{(2)} \end{bmatrix}$

and II_{mnjk}, JJ_{mnjk}, MM_{mnjk} GG_{mnjk}, KK_{mnjk}, fr_{jk} and $f_{jk}^{2,5}$ are matrices whose elements are integrals and function of a_0, β, the form factor $a = H/R$ and the physical properties of the materials. The integrals of all matrix elements are calculated using the recurrence relation of Legendre polynomials.

Eq. (11) gives:

$$\left[IJ_{mnjk} + \Omega^2 MM_{mnjk}\right]p_{m,n}^{(b)} = JK_{mnjk}V_0 \tag{12}$$

where $IJ_{mnjk} = II_{mnjk} - JJ_{mnjk}\left[KK_{mnjk}\right]^{-1} GG_{mnjk}$ and $JK_{mnjk} = JJ_{mnjk}\left[KK_{mnjk}\right]^{-1} f_{jk}^{2,5} - fr_{jk}$.

The developed model allows both harmonic and modal analyses to be performed. It gives direct access to the resonant and anti-resonant frequencies respectively.

Using the displacement current density in the cylindrical piezoelectric resonator defined as $J = i\omega D_z$, the average electrical current I_0 that flows through the metallic electrode of area S is given by:

$$I_0(z) = j\omega\varepsilon_{33}\int\int_{(S)} \overline{D}_z(r,z)\,dS \tag{13}$$

Using the expression of the electrical displacement component D_z defined in equation (3), and calculating the spatial average current I_0 of the partially electroded resonator, we obtain:

$$I_0 = j\omega C_0^{R_0}\left(-V_0 + P1_{mn}\,p_{m,2n}^{(q_1,1)} + P2_{mn}\,p_{m,2n+1}^{(q_3,1)} + P0_{mn}\,p_{m,2n}^{(q_1,2)} + P0_{mn}\,p_{m,2n+1}^{(q_3,2)}\right) \tag{14}$$

where $C_0^{R_0} = \dfrac{\pi R_0^2}{H}\varepsilon_{33}$ is the static capacitance of the partially electroded resonator,

$P0_{mn}$ is the identity matrix with m and n running from zero to respectively M and N,

$$P1_{mn} = \frac{a\beta}{a_0^2}\frac{\overline{e}_{31}}{\overline{\varepsilon}_{33}}\sqrt{2a_0}\left(\int_0^{a_0} Q_0^*(q_1)\,q_1\,\frac{\partial Q_m(q_1)}{\partial q_1}\,dq_1 + \int_0^{a_0} Q_0^*(q_1)\,Q_m(q_1)dq_1 N_{0,m}\right)\int_{-1}^{1} Q_0^*(q_3)\,Q_{2n}(q_3)dq_3$$

and $P2_{mn} = \dfrac{2\beta}{a_0^2}\dfrac{\overline{e}_{33}}{\overline{\varepsilon}_{33}}\sqrt{2a_0}\int_0^{a_0} Q_0^*(q_1)\,q_1\,Q_m(q_1)dq_1 \times \int_{-1}^{1} Q_0^*(q_3)\,\dfrac{\partial Q_{2n+1}(q_3)}{\partial q_3}\,dq_3$

2.1. Harmonic analysis

The objective is now to calculate the normalized electrical input admittance of the micro electromechanical system (MEMS) resonator $\overline{Y}$ expressed in a normalized form as:

$$\overline{Y} = \frac{Y}{j\omega C_0^{R_0}} \tag{15}$$

The expansion of equation (15) gives the normalized electric input admittance:

$$\overline{Y}(\Omega) = 1 - \frac{1}{V_0}\alpha_{m,n}^{(b)} p_{m,n}^{b}(\Omega) \tag{16}$$

where the matrix element factors $\alpha_{m,n}^{(b)}$ (row matrix) and $p_{m,n}^{b}(\Omega)$ (column matrix) can be expressed as: $\alpha_{m,n}^{(b)} = [P1_{mn} \quad P2_{mn} \quad P0_{mn} \quad P0_{mn}]$ and $p_{m,n}^{b}(\Omega) = [\, p_{m,2n}^{(q_1,1)} \quad p_{m,2n+1}^{(q_3,1)} \quad p_{m,2n}^{(q_1,2)} \quad p_{m,2n+1}^{(q_3,2)} \,]^t$.

2.2. Modal analysis: resonance and anti-resonance frequencies

Modal analysis is a specific case of harmonic analysis obtained by cancellation of the electrical excitation. To calculate the resonance frequencies Ω_r, we will cancel the voltage excitation V_0 across the electrodes. In this case, Eq. (12) becomes:

$$\Omega_r^2 p_{m,n}^{(b)} = -\left[MM_{mnjk}\right]^{-1} IJ_{mnjk} p_{m,n}^{(b)} \tag{17}$$

Similarly, for calculating the anti-resonance frequencies Ω_a, we vanish the normalized input admittance in Eq. (16), and substituting in Eq. (12) the voltage excitation source V_0 by the obtained result gives:

$$\Omega_a^2 p_{m,n}^{(b)} = -\left[MM_{mnjk}\right]^{-1}\left[IJ_{mnjk} - JK_{mnjk}\alpha_{m,n}^{(b)}\right] p_{m,n}^{(b)}. \tag{18}$$

3. Numerical results

Based on the foregoing formulations, a computer program was written with Matlab software to numerically calculate the resonance and anti-resonance frequencies through a modal analysis and the normalized electrical input admittance through a harmonic analysis. The physical properties of the materials used in this approach, PIC151 and PZT5A, are presented in the following Table 1. As mentioned above, the summation over the polynomials in Eqs.

(9) and (10) is truncated at some finite values $m = M$ and $n = N$ when higher order terms become negligeable.

3.1. Validation with complete metallization

In this paper, we developed a semi-analytical analysis for modelling MEMS resonators with a voltage excitation using a partial metallization. Two analyses are presented: harmonic analysis for calculating the normalized input electrical admittance of the resonator and modal analysis for calculating the resonance and anti-resonance frequencies. In order to validate our numerical results, these analyses have been validated in the case of a MEMS resonator with a complete metallization for thickness extensional, rod and radial modes for which one-dimensional approached analytical models exist [25]. For the present approach, we simulate a complete metallization by $a_0 = 99\%$.

We used our present polynomial approach to calculate the normalized electric input impedance of a fully electroded PIC151 resonator as a function of the normalized frequency Ω for thickness extensional modes (Fig. 2a), rod modes (Fig. 2b) and radial modes (Fig. 2c). Obtained results are compared with results obtained thanks to a previous software written exclusively for fully electroded resonators [25]. The truncation order is M=N=10. As shown in these figures, our results are in good accordance. Our approach was also initially tested for resonance and anti-resonance frequencies of PIC151 resonator disc respectively for thickness, rod and radial modes. Comparison of our results not reported here with approached analytical method revealed an agreement to six digits.

3.2. Validation with a partially electroded disc: varying pattern of electrodes

3.2.1 Partial metallization $a_0 = 0.5$

To illustrate the capabilities of our present polynomial approach, resonant frequencies $f_r = \frac{1}{2H}\left(\Omega_r \times \sqrt{C_{33}^D / \rho}\right)$ for a MEMS resonator in the form of a partially electroded PZT5A disc with $R_0 = R/2$, R=20.05mm and H=2.03mm were also calculated and compared with those calculated by Guo et al. [30] using a finite element method. The corresponding results are presented in Table 2 with associated accuracies. $\varepsilon_r\% = 100 \times \left| \frac{f_{r\_Guo} - f_{r\_polynomial}}{f_{r\_Guo}} \right|$. A good agreement is obtained.

3.2.2 Partially electroded disc with varying metallization rates

In this section, resonant and anti-resonant frequencies for a MEMS resonator disc were also calculated with several metallization rates. Tables 3 and 4 give respectively a comparison of the resonant f_r and anti-resonant f_a frequencies for an acoustic wave 3D resonator with associated accuracies $\varepsilon_r\% = 100 \times \left| \frac{f_{r\_analytical} - f_{r\_polynomial}}{f_{r\_analytical}} \right|$, $\varepsilon_a\% = 100 \times \left| \frac{f_{a\_analytical} - f_{a\_polynomial}}{f_{a\_analytical}} \right|$ for the metallization rates $a_0 = 0.5$, and 0.7 with R=15mm and H=1mm. A good agreement is obtained between our results using the present polynomial approach and those of an approached analytical model easy to write for thin discs (Appendix A).

To illustrate the capabilities of our polynomial approach with regard to the harmonic analysis for a partially electroded resonator, we have calculated the normalized electric input admittance of the resonator. Fig. 3a and 3b show the calculated normalized admittance for a contour mode PIC151 resonator as a function of the normalized frequency Ω with the metallization rates respectively 60% and 90%. We have also calculated the variation of the frequency parameter $\omega R\sqrt{\rho s_{11}^E\left(1-\upsilon^E\right)^2}$ of the first five extensional resonance modes as a function of the metallization rate a_0 for PIC151 resonator as shown in Fig. 4. The good

agreement obtained between our results calculated by the present polynomial approach and literature results [15] validates our present approach for a partially electroded resonator.

The electromechanical coupling coefficient is an important characteristic of a piezoelectric resonator for converting mechanical energy into electrical energy, or vice versa [15]. This coefficient can be defined as $K^2 = \frac{\sqrt{f_a^2 - f_r^2}}{f_a}$ for $f_a > f_r$, where f_r is the resonance frequency and f_a is the antiresonance frequency for a particular mode. This equation was applied to the appropriate pairs of frequencies f_a, f_r for each mode to calculate the electromechanical coupling coefficient. This coupling coefficient for the first three lowest modes is plotted in Fig. 5 as a function of the metallization rate a_0 for the PIC151 resonator. The results using the present polynomial approach are compared with those published by Chi-Huang [15] for a partially electroded piezoceramic disc. In this presentation, it is clear that the first mode possesses by far the largest coupling of all order modes.

Mechanical displacement modes shapes are characterized by the radial and axial displacements components for longitudinal modes without any circumferential displacement $(u, w \neq 0, v = 0)$. We used our present polynomial approach to calculate the field profiles for a PIC151 partially electroded MEMS resonator. Fig. 6 and 7 depict respectively the radial and axial particle displacement profiles at the resonance frequencies $f_r = 311.369\ kHz$ with a metallization rate 30% and $f_r = 291.675\ kHz$ with a metallization rate 50%. In both cases, the displacement modes shape of the MEMS resonator is dominant under the metallized area.

4. Conclusion

In this paper, we developed a semi-analytical analysis for modelling high contrast partially electroded MEMS resonators. In our model, the Legendre polynomial approach which describes the structure and incorporates automatically the electrical source, the boundary,

symmetry, and continuity conditions in the constitutive and propagation equations is used to calculate the frequency spectrum of a piezoelectric MEMS resonator disc. Two analyses were presented: harmonic analysis for calculating the normalized input electrical admittance and modal analysis for calculating the resonant and anti-resonant frequencies of the resonator. We have also presented as a function of the metallization rate a_0, the electromechanical coupling coefficient and the variation of the frequency parameter of the extensional vibration. The particle displacement profiles are also calculated. The results of our theory are compared with those published earlier in order to check up the accuracy and range of applicability of the proposed approach. The developed software proves to be very efficient to retrieve the resonance and anti-resonance frequencies and the modes of all orders.

Appendix A: For a completely electroded thin disc (H<<R), a one-dimensional approached analytical model easy to write allows to calculate the analytical normalized admittance used to validate our present polynomial approach written for partially electroded resonator:

$$\overline{Y} = 1 + \frac{\left(\frac{d_{31}}{s_{11}^E\left(1-\upsilon^E\right)}\right)^2}{\varepsilon_{33}^T + 2g_{31}d_{31}} J_1(\alpha R_0)\ Minv(1,3)$$

where:

$$M = \begin{pmatrix} J_1(\alpha R_0) & -J_1(\eta R_0) & -Y_1(\eta R_0) \\ 0 & B_0.\eta R.J_0(\eta R) - \frac{J_1(\eta R)}{s_{11}^E\left(1+\upsilon^E\right)} & B_0.\eta R.Y_0(\eta R) - \frac{Y_1(\eta R)}{s_{11}^E\left(1+\upsilon^E\right)} \\ \frac{\alpha R_0.J'_1(\alpha R_0) + \upsilon^E J_1(\eta R_0)}{s_{11}^E\left(1+\upsilon^E\right)^2} & -\left(B_0.\eta R_0.J_0(\eta R_0) - \frac{J_1(\eta R_0)}{s_{11}^E\left(1+\upsilon^E\right)}\right) & -\left(B_0.\eta R_0.Y_0(\eta R_0) - \frac{Y_1(\eta R_0)}{s_{11}^E\left(1+\upsilon^E\right)}\right) \end{pmatrix}$$

$$B_0 = \frac{2-\left(1-\upsilon^E\right)k_p^2}{2s_{11}^E\left(1-\upsilon^E\right)^2\left(1-k_p^2\right)}\ ;\ \alpha R_0 = \omega R_0\sqrt{\rho s_{11}^E\left(1-\upsilon^E\right)^2}\ ;\ \eta R = \omega R\sqrt{\rho\frac{2s_{11}^E\left(1-\upsilon^E\right)^2\left(1-k_p^2\right)}{2-\left(1-\upsilon^E\right)k_p^2}};\ \upsilon^E = -\frac{s_{12}^E}{s_{11}^E}$$

$$\eta R_0 = \omega R_0\sqrt{\rho\frac{2s_{11}^E\left(1-\upsilon^E\right)^2\left(1-k_p^2\right)}{2-\left(1-\upsilon^E\right)k_p^2}},\ J'_1(\alpha R_0) = J_0(\alpha R_0) - \frac{1}{\alpha R_0}J_1(\alpha R_0),\ g_{31} = -\frac{d_{31}}{s_{11}^E\left(1-\upsilon^E\right)}\ ;\ k_p^2 = \frac{2d_{31}^2}{\left(1-\upsilon^E\right)s_{11}^E\varepsilon_{11}^T}$$

where J_0 and J_1 are the Bessel functions of the first kind, s_{11}^E and s_{12}^E are the elastic compliance constants at constant electrical field. g_{31} and d_{31} are the piezoelectric constants, υ^E is the Poisson ratio and ε_{33}^T is the dielectric constant at constant stress. Minv is the inverse matrix of the M matrix.

References

[1] K. Wang, Y. Yu, A. C. Wong, C.T.C. Nguyen, VHF free-free beam high-Q micromechanical resonators, Proceedings of the IEEE International Conference on Micro Electro Mechanical Systems (MEMS) (1999) 453-458.

[2] J. R. Clark, W. T. Hsu, C.T.C. Nguyen, High-Q VHF micromechanical contour-mode disc resonators, IEEE Int Electron Devices Meeting (2000) 493-496.

[3] S. Trolier-Mckinstry, and P. Muralt, Thin Film Piezoelectrics for MEMS, J. Electroceramics, 12 (2004) 7-17.

[4] T. Xu, G. Wu, G. Zhang, Y. Hao, The compatibility of ZnO piezoelectric film with micromachining process, Sensors and Actuators A : Physical, 104 (2003) 61-67.

[5] S. Humad, R.Abdolvand, G.K.Ho, G.Piazza, F.Ayazi, High frequency micromechanical piezo-on-silicon block resonators, IEDM, (2003) 957-960.

[6] R. N. Torah, S. P. Beeby, M. J. Tudor, and N. M. White, Thick-film piezoceramics and devices, Journal of Electroceramics 19 (2007) 97-112.

[7] P. Maréchal, F. Levassort, J. Holc, L. P. Tran-Huu-Hue, M. Kosec, M. Lethiecq, High-frequency transducers based on integrated piezoelectric thick films for medical imaging, IEEE Trans. Ultrason, Ferroelectr Frequency Control 53 (2006) 1524-1533.

[8] J. Hernando, J. L. Sanchez-Rojas, U. Schmid, A. Ababneh, G. Marchand and H. Seidel, Characterization and displacement control of low surface-stress AlN-based piezoelectric micro-resonators, Microsystems Technologies 16 (2010) 855-861.

[9] H. F. Tiersten, Linear piezoelectric plate vibration (Plenum, New York, 1969).

[10] IEEE Standard on Piezoelectricity, ANSI-IEEE Std. 176, IEEE New York, 1987.

[11] N. Guo, P. Cawley and D. Hitchings, The finite element analysis of the vibration characteristics of piezoelectric disc, J. Sound Vib 159 (1992) 115-138.

[12] N. F. Ivina, Numerical analysis of the normal modes of circular piezoelectric plates of finite dimensions, Soviet Physics Acoustics 35 (1990) 385-388.

[13] G. H. Schmidt, Extensional vibrations of piezoelectric plates, J. Eng. Math. 6 (1972), 133-142.

[14] N. N. Rogacheva, The dependence of the electromechanical coupling coefficient of piezoelectric elements on the position and size of the electrodes, J. Appl Math and Mech 0021-8928, 65 (2001) 317-326

[15] C. H. Huang, Theoretical and experimental vibration analysis for a piezoceramic disk partially covered with electrodes, J. Acoust Soc Am 118(2) (2005) 751-761.

[16] S. Datta and B.J. Hunsinger, Analysis of surface waves using orthogonal functions, J. Appl. Phys. 49 (1978) 475-479.

[17] J. E. Lefebvre, V. Zhang, J. Gazalet, T. Gryba and V. Sadaune, Acoustic Waves Propagation in Continuous Functionally Graded Plates: An Extension of the Legendre Polynomial Approach, IEEE Trans. Ultrason. Ferroelectr. Frequency Control 48 (5) (2001) 1332-1340.

[18] J. E. Lefebvre, V. Zhang, J. Gazalet and T. Gryba, Legendre polynomial approach for modelling free ultrasonic waves in multilayered plates, J. Appl. Phys. 85 (7) (1999) 3419-3427.

[19] L. Elmaimouni, J. E. Lefebvre, V. Zhang and T. Gryba, Guided waves in inhomogeneous cylinders of Functionally Graded Materials (FGM), NDT and E Int 38 (5) (2005) 344-353.

[20] J. Yu, J. E. Lefebvre, Y. Guo, and L. Elmaimouni, Wave Propagation in the Circumferential Direction of General Multilayered Piezoelectric Cylindrical Plates, IEEE Trans. Ultrason. Ferroelectr. Frequency Control 59 (2012) 2498-2508.

[21] J. G. Yu. J. E. Lefebvre and L. Elmaimouni, Toroidal wave in multilayered spherical curved plates, J. Sound Vib 332 (2013) 2816-2830.

[22] L. Elmaimouni, J. E. Lefebvre, A. Raherison and F. E. Ratolojanahary, Acoustical Guided Waves in Inhomogeneous Cylindrical Materials, Ferroelectrics (Taylor and Francis Group) 372 (2008) 115-123.

[23] L. Elmaimouni, J. E. Lefebvre, F. E. Ratolojanahary, A. Raherison, T. Gryba and J. Carlier, Modal analysis and harmonic response of resonators: an extension of a mapped orthogonal functions technique, Wave Motion 48 (2011) 93-104.

[24] L. Elmaimouni, J. E. Lefebvre, F. E. Ratolojanahary A. Raherison, B. Bahani and T. Gryba, Polynomial approach modeling of resonator piezoelectric disc, Key Eng. Materials, Dynamics of the structures and Non Destructive testing 1294, (2011) 11-20.

[25] L. Elmaimouni, F. E. Ratolojanahary, J. E. Lefebvre, J.G. Yu, A. Raherison and T. Gryba, Modeling of MEMS resonator piezoelectric disc by means of an equicharge current source method, Ultrasonics 53 (2013) 1270-1279.

[26] A. Raherison, F. E. Ratolojanahary, J. E. Lefebvre, L. Elmaimouni, Legendre polynomial modeling of composite BAW resonators, J. Appl. Phys. 104 (2008) 014508.

[27] A. Raherison, J. E. Lefebvre, F. E. Ratolojanahary, L. Elmaimouni and T. Gryba, 2D Legendre polynomial modeling of composite bulk acoustic wave resonators, J. Appl. Phys. 108 (2010) 104904.

[28] P. M. Rabotovao, F. E. Ratolojanahary, J. E. Lefebvre, A. Raherison, L. Elmaimouni, T. Gryba, and J. G. Yu, Modeling of high contrast partially electroded resonators by means of a polynomial approach, J. Appl. Phys. 114 (2013) 124502.

[29] B.A. Auld, Acoustic Fields and Waves in Solids, Krieger, Malabar, FL, 1990.

[30] N. Guo, The vibration characteristics of piezoelectric discs, Dissertation, Department of Mechanical Engineering, Imperial College of Science, Technology and Medicine, London, 1989.

Table(s)

Table 1

Material properties used in simulations for PIC151 and PZT5A piezoelectric resonator discs.

Parameters	PIC151	PZT5A
Elastic Stiffness at constant electric field E $(\times 10^{11}\ N/m^2)$		
C_{11}	1.0760	1.21
C_{12}	0.6313	0.754
C_{13}	0.6386	0.752
C_{33}	1.0041	1.11
C_{55}	0.1962	0.211
$C_{66}=(C_{11}- C_{12})/2$	0.2224	0.226
Piezoelectric constant $(C.m^{-2})$		
e_{15}	11.9702	12.3
e_{31}	-9.5226	-5.4
e_{33}	15.1393	15.8
Permittivity at constant strain $(\times 10^{-11}\ F.m^{-1})$		
ε_{11}	983.219	811.026
ε_{33}	818.542	734.88
Mass density $(10^3\ Kg.m^{-3})$		
ρ	7.800	7.750

Table(s)

Table 2

Normalized resonance frequencies of first six rod modes of a partially metallized PZT5A piezoelectric resonator

Mode	Partially electroded disc		ε_r%
	f_{r_Guo}(kHz) [30]	$f_{r\_polynomial}$(kHz)	
1	53.74	53.64	0.1861
2	140.6	140.78	0.1280
3	215.8	215.54	0.1205
4	295.5	295.68	0.0609
5	364.5	363.67	0.2277
6	431.6	432.11	0.1182

Table(s)

Table 3

Normalized resonance and anti-resonance frequencies of first five radial modes of a partially electroded PIC151 piezoelectric resonator disc with $a_0 = 0.5$

	Resonance frequency			Anti-resonance frequency		
Mode	$f_{r\_analytical}$ (kHz)	$f_{r\_polynomial}$ (kHz)	ε_r%	$f_{a\_analytical}$ (kHz)	$f_{a\_polynomial}$ (kHz)	ε_a%
1	71.732	71.757	0.0349	84.293	84.331	0.0451
2	189.636	189.742	0.0559	195.042	195.256	0.1097
3	291.586	291.675	0.0305	295.914	296.217	0.1024
4	406.851	406.979	0.0315	408.011	408.442	0.1056
5	508.965	509.312	0.0682	512.447	512.968	0.1017

Table(s)

Table 4

Normalized resonance and anti-resonance frequencies of first five radial modes of a partially electroded PIC151 piezoelectric resonator disc with $a_0 = 0.7$

	Resonance frequency			Anti-resonance frequency		
Mode	$f_{r\_analytical}$ (kHz)	$f_{r\_polynomial}$ (kHz)	$\varepsilon_r\%$	$f_{a\_analytical}$ (kHz)	$f_{a\_polynomial}$ (kHz)	$\varepsilon_a\%$
1	67.198	67.221	0.0327	83.503	83.615	0.1341
2	178.315	178.421	0.0594	178.617	178.843	0.1265
3	286.670	286.786	0.0405	288.139	288.454	0.1093
4	387.758	387.865	0.0276	391.387	391.790	0.1030
5	487.643	487.859	0.0443	489.303	489.868	0.1155

Figure(s)

Figure captions

Fig. 1 Configuration of partially electroded piezoelectric resonator disc

Fig. 2 Normalized electric input impedance of PIC151 resonator for (a) thickness extensional modes, (b) rod modes, and (c) radial modes (M=N=10) [25]

Fig. 3 Normalized electric input admittance of PIC151 resonator as a function of normalized frequency of contour modes with (a) metallization rate of 60%, (b) metallization rate of 90%

Fig. 4 Variation in frequency parameter of first five extensional resonance modes as a function of the metallization rate a_0 for the PIC151 piezoelectric resonator

Fig. 5 Electromechanical coupling coefficients for the PIC151 piezoelectric resonator as a function of the metallization rate a_0 (∗ *polynomial results*, *solid lines: results from C. H. Huang et al*)

Fig. 6 Radial and axial displacement profiles for a PIC151 resonator with a metallization rate of 30% at the resonance frequency $f_r = 311.369\ kHz$

Fig. 7 Radial and axial displacement profiles for a PIC151 resonator with a metallization rate of 50 % at the resonance frequency $f_r = 291.675\ kHz$

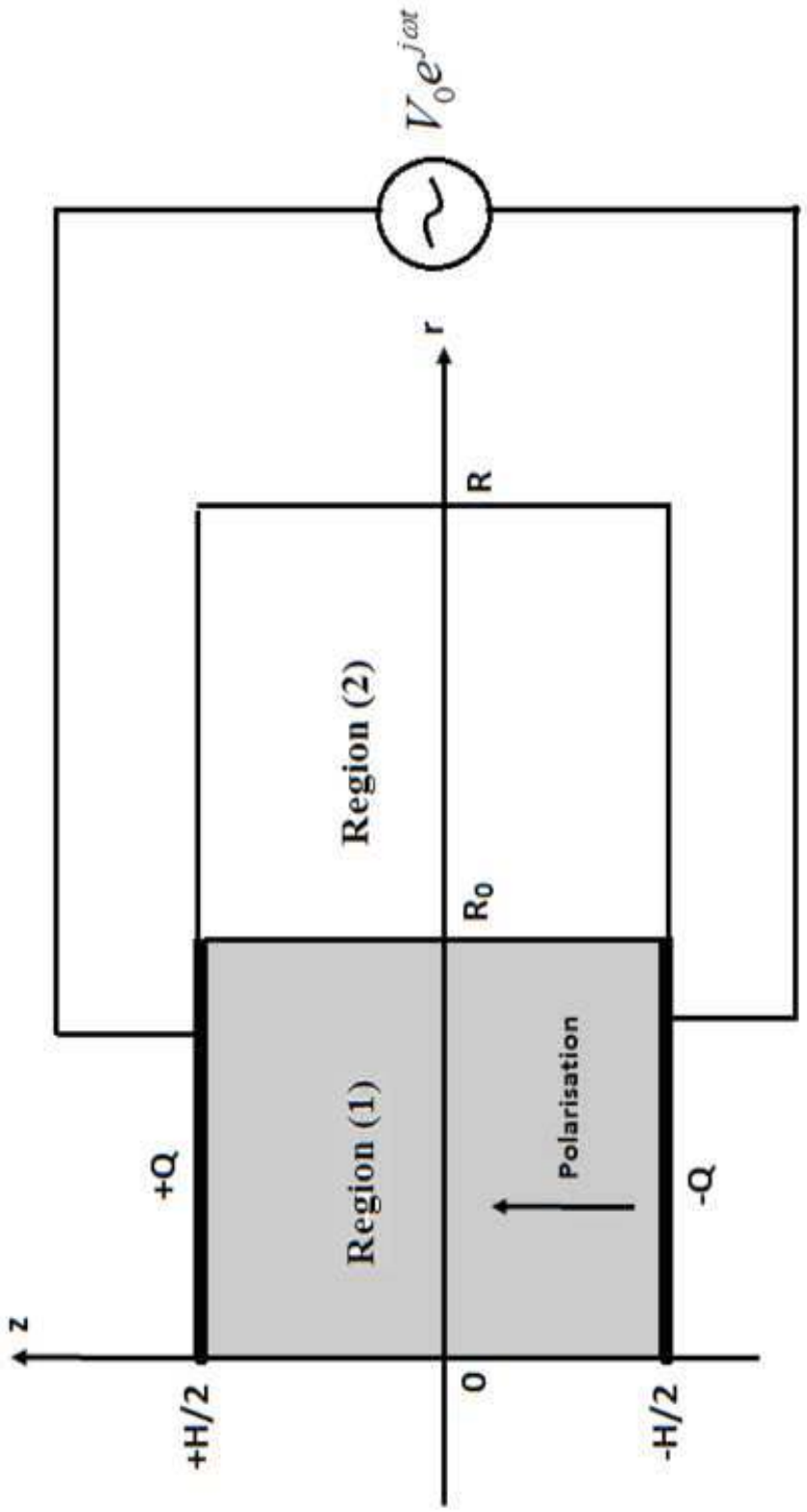
$V_0 e^{j\omega t}$
r
R
R_0
Region (2)
Region (1)
Polarisation
+Q
-Q
z
+H/2
0
-H/2

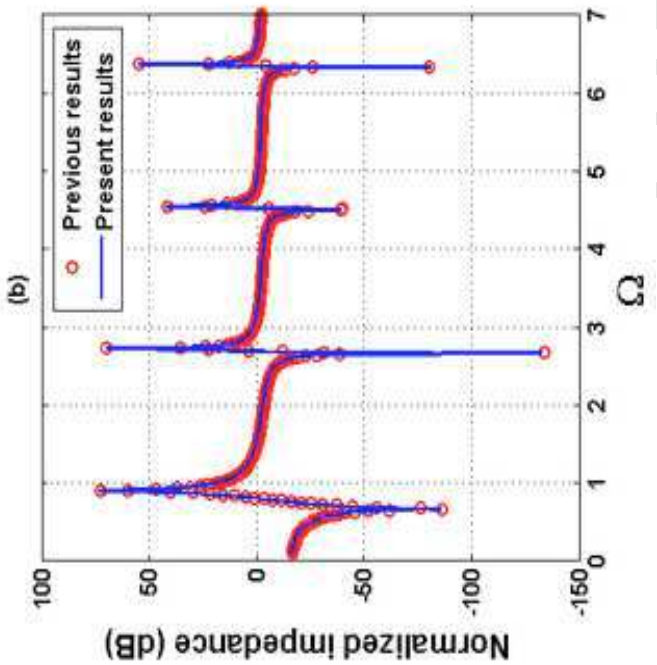

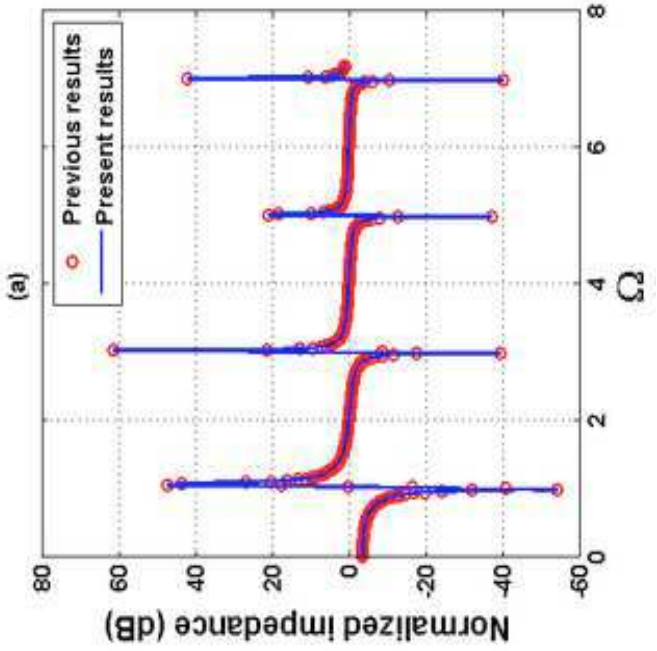

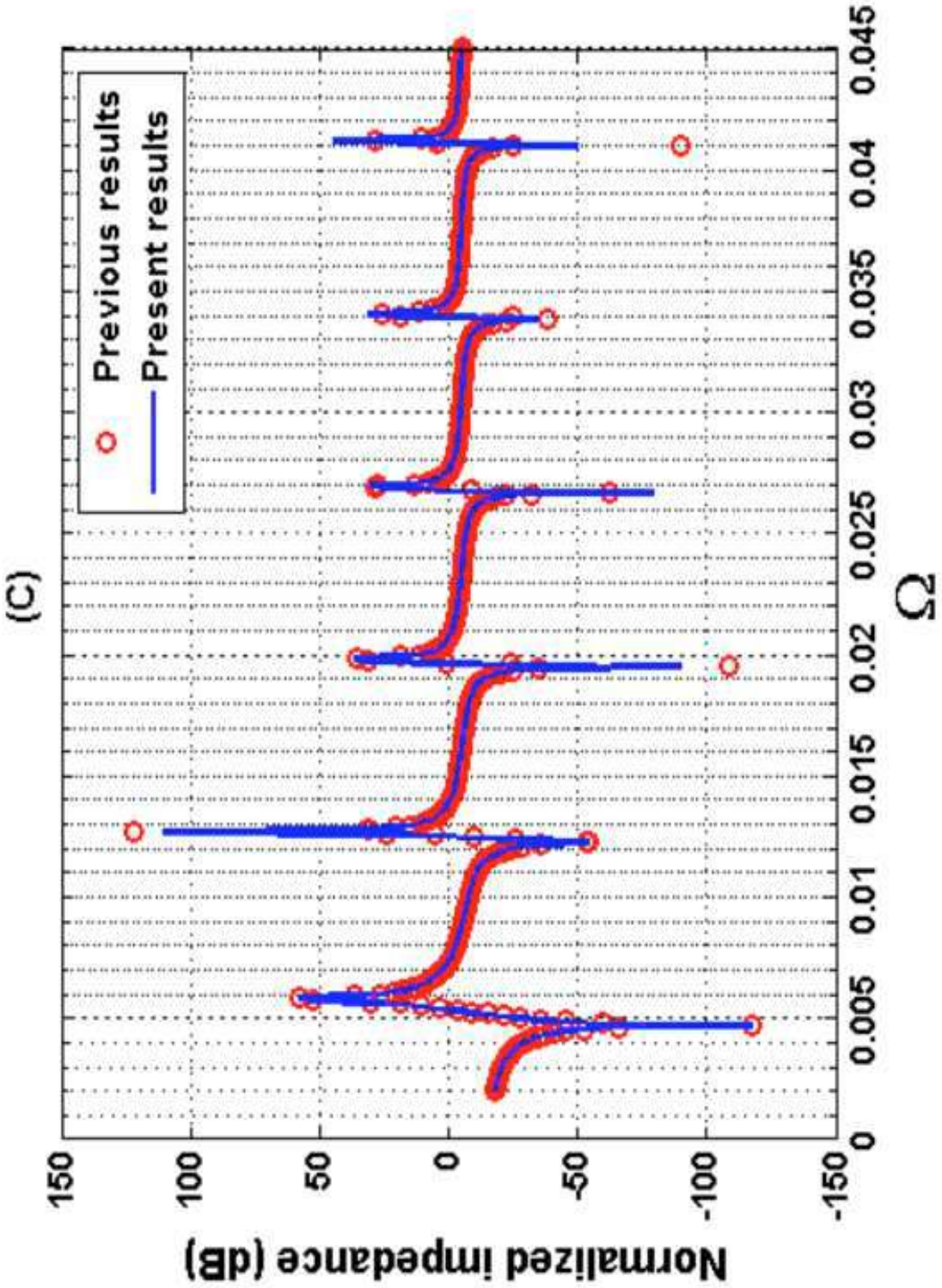

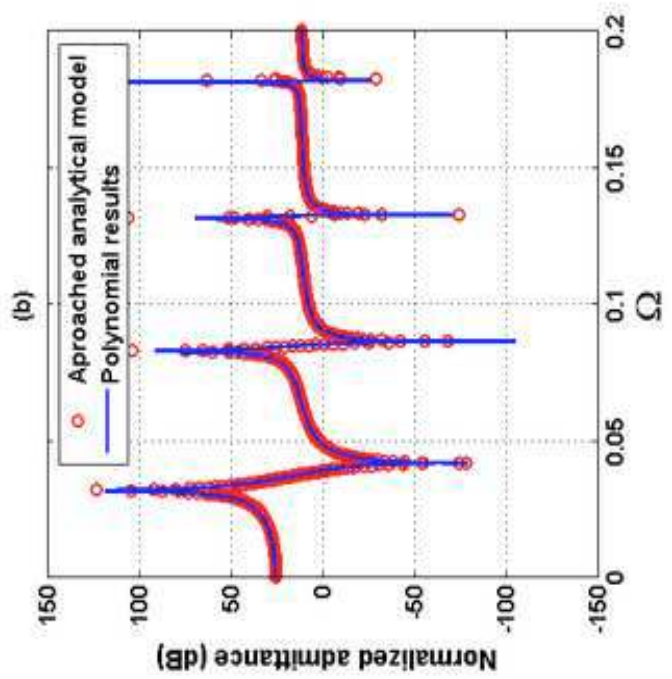

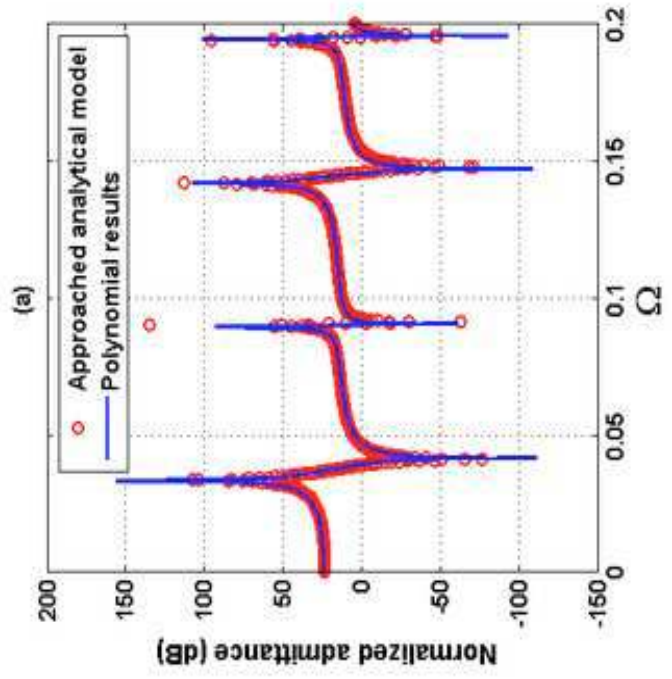

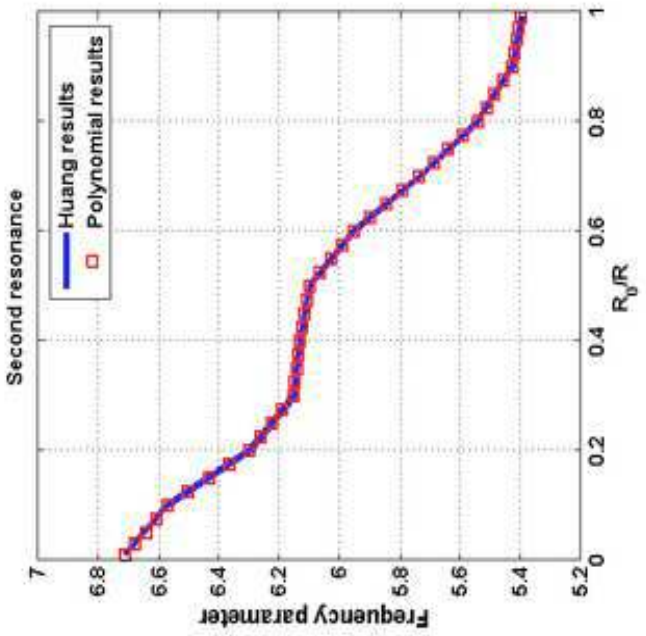

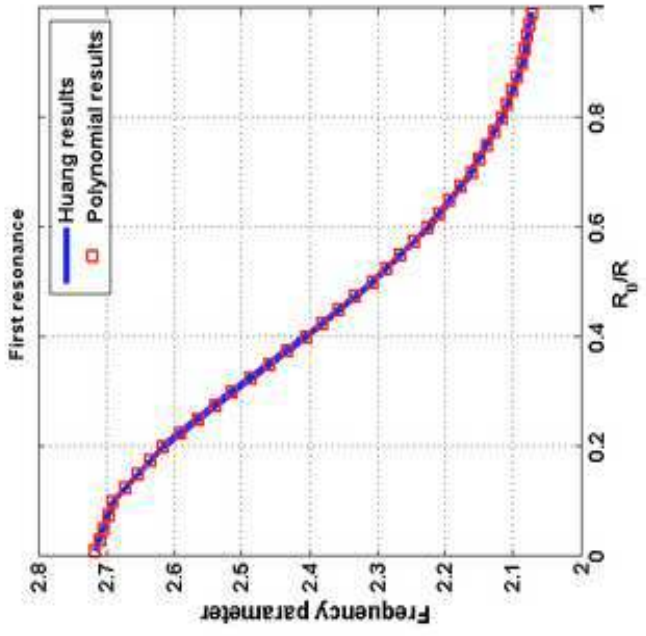

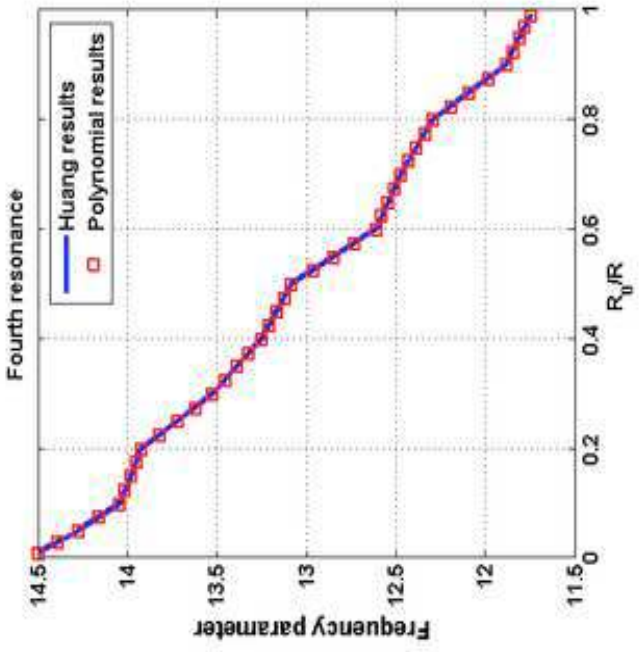

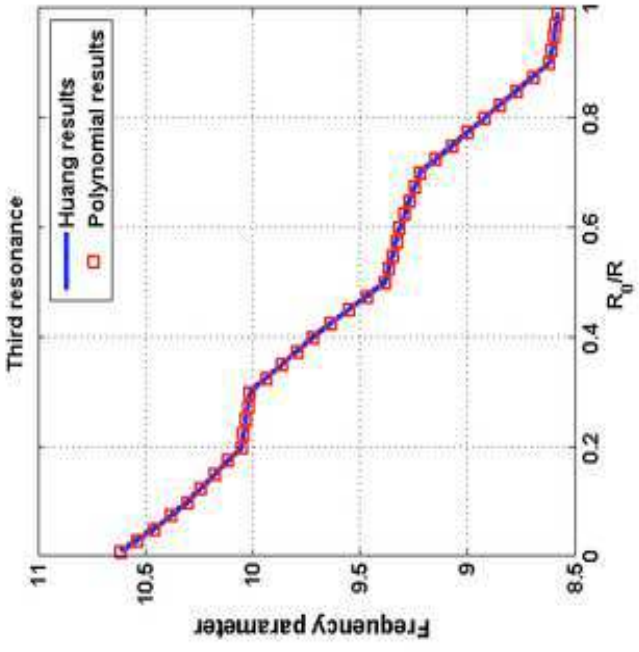

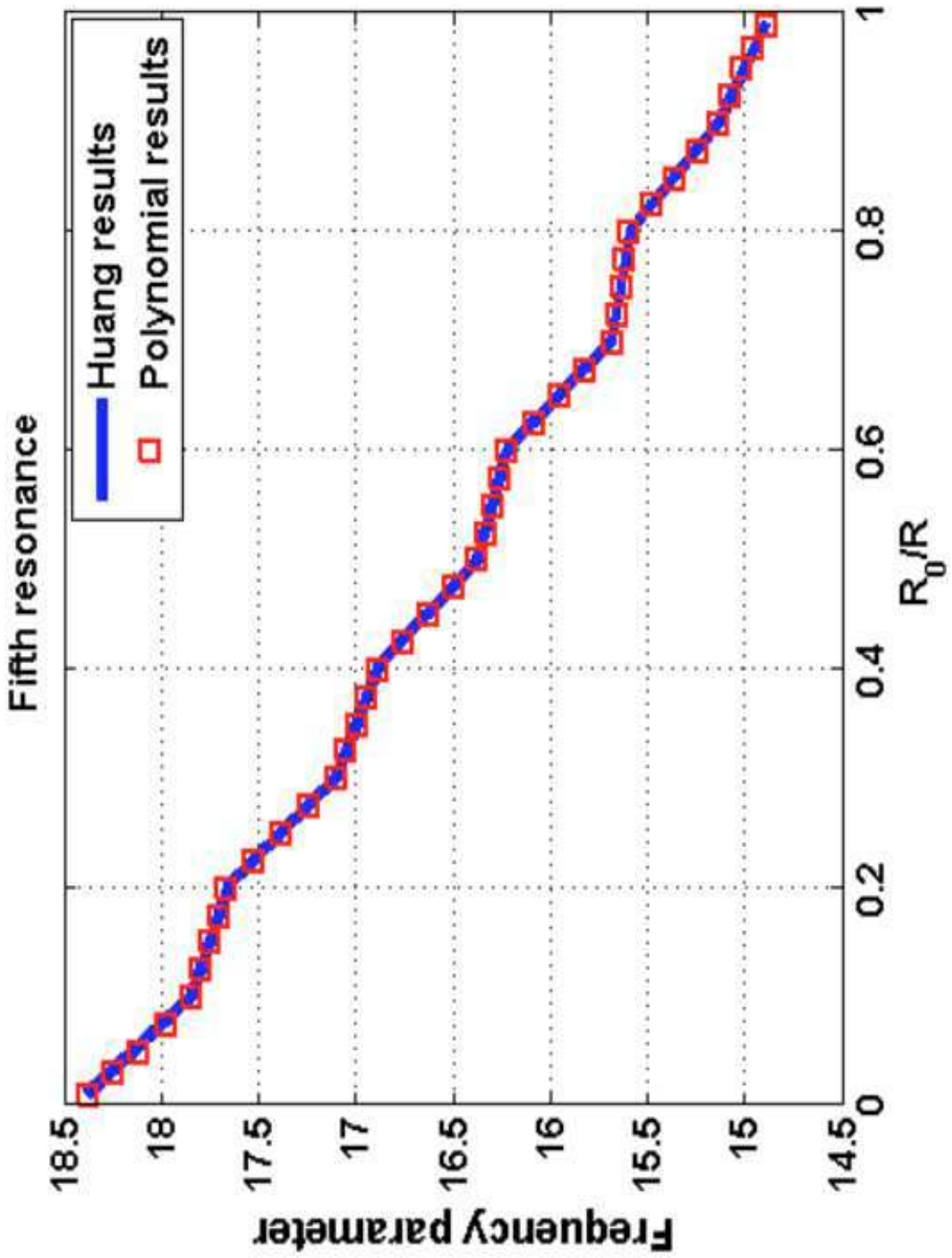
Fifth resonance
Huang results
Polynomial results
Frequency parameter
R_0/R
18.5
18
17.5
17
16.5
16
15.5
15
14.5
0
0.2
0.4
0.6
0.8
1

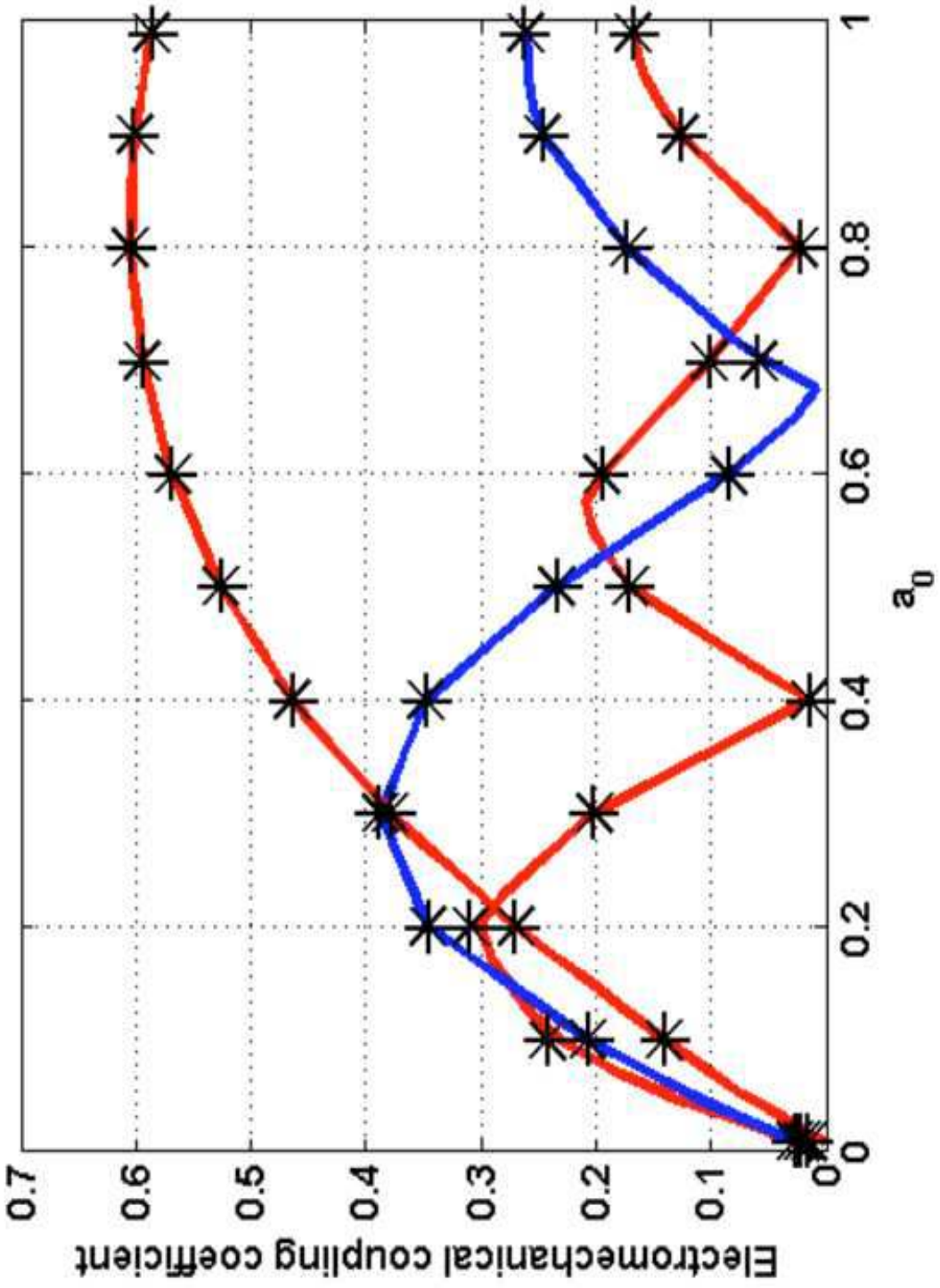
Electromechanical coupling coefficient
0.7
0.6
0.5
0.4
0.3
0.2
0.1
0
0.2
0.4
0.6
0.8
1
a_0

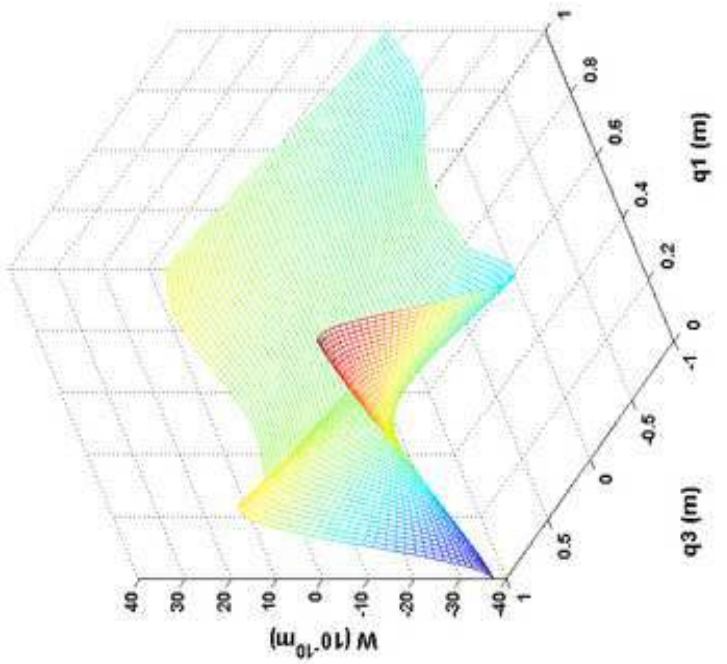
W (10^-10 m)
40
30
20
10
0
-10
-20
-30
-40
1
0.5
0
-0.5
-1
q3 (m)
0
0.2
0.4
0.6
0.8
1
q1 (m)

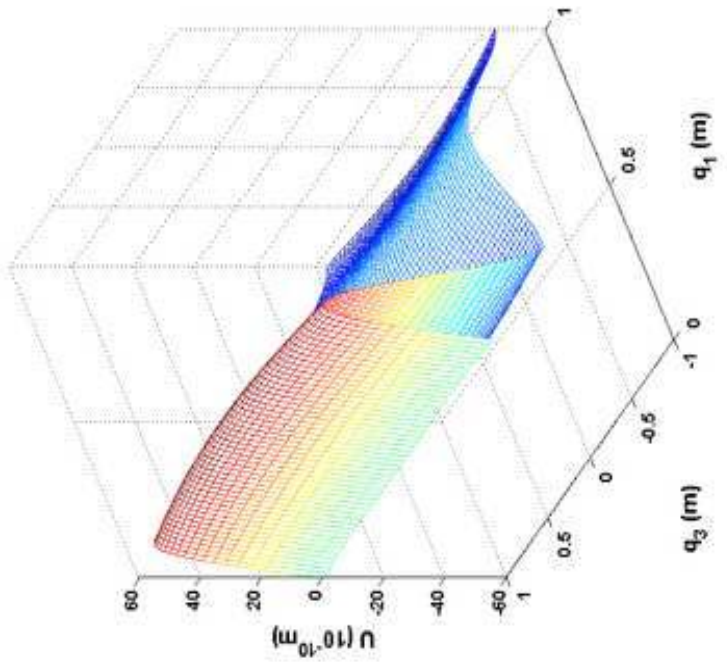
U (10^-10 m)
60
40
20
0
-20
-40
-60
1
0.5
0
-0.5
-1
q3 (m)
0
0.5
1
q1 (m)

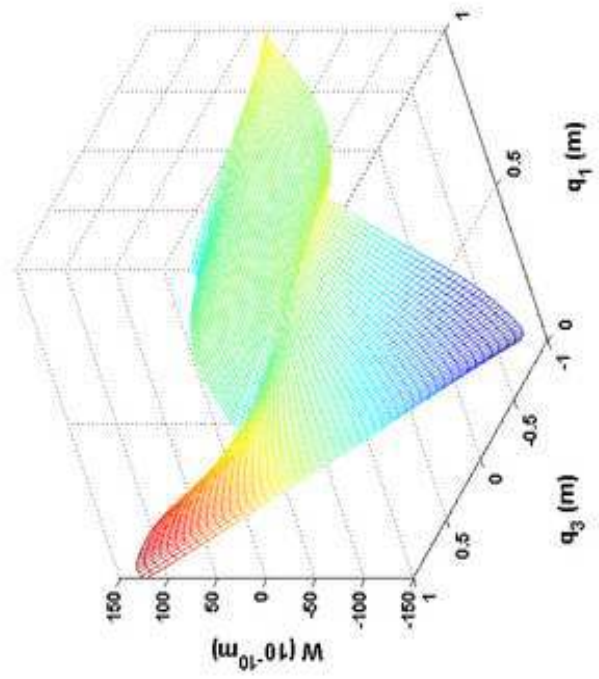
W (10^-10 m)
150
100
50
0
-50
-100
-150
q3 (m)
1
0.5
0
-0.5
-1
q1 (m)
1
0.5
0
-0.5
-1

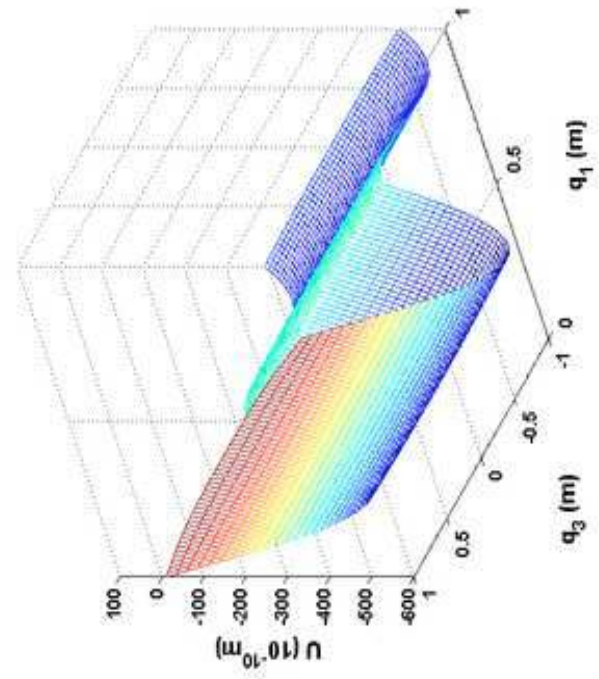
U (10^-10 m)
100
0
-100
-200
-300
-400
-500
-600
q3 (m)
1
0.5
0
-0.5
-1
q1 (m)
1
0.5
0
-0.5
-1